Published in final edited form as:
Angiogenesis. 2013 January ; 16(1): 45–58. doi:10.1007/s10456-012-9298-5.

Estradiol promotes neural stem cell differentiation into endothelial lineage and angiogenesis in injured peripheral nerve

Haruki Sekiguchi,
Feinberg Cardiovascular Research Institute, Northwestern University Feinberg School of Medicine, Chicago, IL, USA

Department of Cardiology, Aoyama Hospital, Tokyo Women's Medical University, Tokyo, Japan

Department of Cardiology, National Hospital Organization Yokohama Medical Center, Kanagawa, Japan

Masaaki Ii,
Department of Pharmacology, Faculty of Medicine, Osaka Medical College, 2-7, Daigaku-machi, Takatsuki, 569-8686 Osaka, Japan

Kentaro Jujo,
Feinberg Cardiovascular Research Institute, Northwestern University Feinberg School of Medicine, Chicago, IL, USA

Department of Cardiology, Tokyo Women's Medical University, Tokyo, Japan

Tina Thorne,
Feinberg Cardiovascular Research Institute, Northwestern University Feinberg School of Medicine, Chicago, IL, USA

Aiko Ito,
Feinberg Cardiovascular Research Institute, Northwestern University Feinberg School of Medicine, Chicago, IL, USA

Ekaterina Klyachko,
Feinberg Cardiovascular Research Institute, Northwestern University Feinberg School of Medicine, Chicago, IL, USA

Hiromichi Hamada,
Departments of Pediatrics and Pediatric Intensive Care Medicine, Yachiyo Medical Center, Tokyo Women's Medical University, Chiba, Japan

John A. Kessler,
Department of Neurology, Northwestern University Feinberg School of Medicine, Chicago, IL, USA

Yasuhiko Tabata,
Department of Biomaterials, Field of Tissue Engineering, Institute for Frontier Medical Sciences, Kyoto University, Kyoto, Japan

Correspondence to: Masaaki Ii, masa0331@mac.com.

Electronic supplementary material The online version of this article (doi:10.1007/s10456-012-9298-5) contains supplementary material, which is available to authorized users

Conflict of interest Douglas W. Losordo, MD has significant relationships as PI, collaborator or consultant with the following companies: AccelRX, Arsenal, Biomedical, BioCardia, Genzyme, Baxter Healthcare Corp., Cordis, NeoStem, and Viromed.

Masatoshi Kawana,
Department of Cardiology, Aoyama Hospital, Tokyo Women's Medical University, Tokyo, Japan

Department of Cardiology, Tokyo Women's Medical University, Tokyo, Japan

Michio Asahi,
Department of Pharmacology, Faculty of Medicine, Osaka Medical College, 2-7, Daigaku-machi, Takatsuki, 569-8686 Osaka, Japan

Nobuhisa Hagiwara, and
Department of Cardiology, Tokyo Women's Medical University, Tokyo, Japan

Douglas W. Losordo
Feinberg Cardiovascular Research Institute, Northwestern University Feinberg School of Medicine, Chicago, IL, USA

Masaaki Ii: masa0331@mac.com

Abstract

Neural stem cells (NSCs) differentiate into endothelial cells (ECs) and neuronal cells. Estradiol (E2) is known to exhibit proangiogenic effects on ischemic tissues via EC activation. Therefore, we hypothesized that E2 can promote the therapeutic potential of NSC transplantation for injured nerve repair via the differentiation of NSCs into ECs during neovascularization. NSCs isolated from newborn mouse brains were transplanted into injured sciatic nerves with (NSC/E2 group) or without E2-conjugated gelatin hydrogel (E2 group). The NSC/E2 group exhibited the greatest recovery in motor nerve conduction velocity, voltage amplitude, and exercise tolerance. Histological analyses revealed increased intraneural vascularity and blood perfusion as well as striking NSC recruitment to the neovasculature in the injured nerves in the NSC/E2 group. In vitro, E2 enhanced the NSC migration and proliferation inhibiting apoptosis. Fluorescence-activated cell sorting analysis also revealed that E2 significantly increased the percentage of CD31 in NSCs, and the effect of E2 was completely neutralized by the estrogen receptor antagonist ICI. The combination of E2 administration and NSC transplantation cooperatively improved the functional recovery of injured peripheral nerves, at least in part, via E2-associated NSC differentiation into ECs. These findings provide a novel mechanistic insight into both NSC biology and the biological effects of endogenous E2.

Keywords

Estrogen; Neural stem cell; Cell transplantation; Angiogenesis; Endothelial differentiation; Nervous system

Introduction

The gonadal steroid 17β-estradiol (E2), also known as biologically active estrogen, is an important female sex hormone. Recent studies have revealed that it also influences the development, growth, differentiation, maturation, and function of the central nervous system (CNS); in addition, it plays a role in neuroprotection [1]. E2 protects cultured primary neurons against the neurotoxic effects of glutamate [2] and oxidative stress [3], and it's neuroprotective effects are also observed in vivo. Animal studies have revealed that in the event of high E2 levels during the premenopausal period, female rodents are reportedly less vulnerable to acute insults, such as cerebral ischemia [4] and neurotrauma [5].

Neurospheres are free-floating heterogeneous aggregates that contain a minority of neural stem cells (NSCs) together with various progenitors and more differentiated cells. These

clusters of cells, under appropriate culture conditions, can produce neurons, astrocytes, and oligodendrocytes [6–9]. Neurosphere-derived cells have been successfully used in models of brain injury, such as experimental autoimmune encephalomyelitis or spinal cord injury [6, 10–12].

Recent studies have indicated that NSCs can differentiate into both neurons and endothelial cells (ECs), and the ability of NSCs to differentiate into ECs has been demonstrated in vitro [13] and in vivo [24]. Conversely, researchers from our lab as well as others have previously revealed that E2 favorably affects angiogenesis after ischemic nerve injury [14–16]; furthermore, it can reportedly participate in the nerve recovery process [17, 18].

E2 administration and NSC transplantation have been investigated as modalities for the treatment of ischemic tissues and cerebral ischemia. In cases of peripheral nerve injury, they stimulate angiogenesis and neurogenesis during the process of recovery from nerve damage.

In the present study, we explored the potential effectiveness of combined E2 and NSC therapy for peripheral nerve injury. We hypothesized that combination therapy comprising agents that enhance neurogenesis as well as angiogenesis is beneficial compared to monotherapy. We used E2 for the enhancement of angiogenesis in our study.

However, systemic treatment with E2 is associated with several problems such as breast carcinogenesis, and systemic stem cell injection is also problematic because of adverse effects on other organs. To prevent these systemic side effects, we selected local NSC transplantation in combination with slow-release E2 as a therapy for injured nerves.

In this study, we used a murine model of peripheral nerve injury to investigate whether E2 and NSC combination therapy decreased sciatic nerve injury and stimulated recovery of nerve function, whether transplanted NSCs could differentiate into ECs, and whether E2 promoted NSC differentiation into ECs.

Methods

Drugs

E2-poly-d,l-lactide-co-glycolide (E2-PLGA) was provided by Dr. Tabata (Kyoto University, Japan). The weight-averaged molecular weight of PLGA was approximately 23,000, and the monomer composition was 50 mol % lactide and 50 mol % glycolide. E2 was purchased from Tokyo Kasei Kogyo Co. Ltd. Polyvinyl alcohol 500 was purchased from Kishida Chemicals. The estrogen receptor antagonist ICI 128780 was obtained from Tokris Cookson (Bristol, UK). E2 pellets (0.5 mg/60-day release) were purchased from Innovative Research of America (Sarasota, FL) and implanted subcutaneously in mice only for the measurement of serum E2 levels comparing with local administration of PLGA microspheres containing E2. The 5-Bromo-2′-deoxyuridine (BrdU) was purchased from Sigma-Aldrich. (St. Louis, MO) BrdU is incorporated into cellular DNA during cell proliferation.

Preparation of PLGA microspheres containing E2

PLGA microspheres containing E2 were used without emulsion as previously described [19].

Animal protocol

The Institutional Animal Care and Use Committee of Northwestern University approved all described studies. This study was designed to investigate the effects of NSC and E2 combination therapy on recovery in injured peripheral nerves. Neural stem cells were isolated from neonatal C57BL/6 J or enhanced green fluorescent protein mice [20] of either

sex. To compare local versus systemic effect of E2 on neural regeneration, E2 pellets (Innovative Research of America, Sarasota, FL, USA) was subcutaneously implanted in wild-type recipient female mice 1 week before surgery as systemically E2 administration group. Wild-type recipient female mice were subjected to unilateral sciatic nerve crush injury, following which the mice were randomized to one of 4 treatments ($n = 5$ each): E2 administered locally via the biodegradable polymer PLGA (E2-PLGA), NSC administered locally via the biodegradable polymer PLGA (NSC-PLGA), a combination of E2-PLGA and NSC treatments, and PLGA monotherapy (control).

Neural progenitor cell culture

Medial, lateral, and caudal ganglionic eminences dissected from postnatal day 1 pups (C57BL/6 J mice, Jackson Laboratory) were dissociated and digested enzymatically with 0.05 % trypsin/0.53 mM EDTA (Invitrogen, Carlsbad, CA) for 5 min at 37 °C. Trypsin activity was inhibited by adding soybean trypsin inhibitor (2.8 mg/mL, Roche Diagnosis, Mannheim, Germany). After washing with DMEM/F-12 (1:1), the tissue samples were triturated using a fire-polished Pasteur pipette and passed through a 40-μm nylon mesh (Cell Strainer, Becton–Dickinson, Franklin Lakes, NJ) to obtain single-cell suspensions. Then the cells were seeded at an initial cell density of 1×10^5 cells/mLin NeuroCult® NSC Basal Medium (StemCell Technologies) supplemented with 1 % N2 (Invitrogen), 1 % B27 (Invitrogen), epidermal growth factor (20 ng/mL; Peprotech Inc. Rocky Hill, NJ), basic fibroblast growth factor 2 (10 ng/mL; Peprotech Inc.), and a 1/10 dilution of NeuroCult® NSC Proliferation Supplements (StemCell Technologies). After approximately 4 days of culture, the cells formed primary neurospheres, which were dissociated into single NSCs using a NeuroCult Chemical Dissociation kit (StemCell Technologies), plated at a density of 5×10^4 cells/mL, and grown for 4 days until secondary neurospheres formed. The cells were passaged every time the cells formed neurospheres. NSCs were labeled by CM-DiI (Invitrogen) as previously described [21].

Differentiation of neural progenitor cells

Secondary neural progenitor cells were dissociated using a NeuroCult® Chemical Dissociation kit (StemCell Technologies) and plated at 50,000 cells/mL on poly-D-lysine (Sigma) and laminin (Sigma)-coated glass coverslips. The cells were maintained for 7 days in NeuroCult® NSC Basal Medium (StemCell Technologies) supplemented with 1 % N2, 1 % B27, 1 % calf serum, and NeuroCult® NSC Differentiation Supplements prior to fixation and staining for lineage markers (microtubule-associated protein, glial fibrillary acidic protein, oligodendrocyte marker O4, and nestin).

Proliferation assay, migration assay and anti-apoptosis assays

The assays for NSCs bioactivity affected by E2 were performed, as described previously [1, 2]. For proliferation assay, five thousands of NSCs cultured in the 96 well plates with NSC proliferation medium with several concentrations of E2. After 48 h, the cells were added MTS solution (DOJINDO, Japan) and measured according to the manufacturer's instructions. For anti-apoptosis assay (TUNEL labeling), one thousands of NSCs were cultured under several conditions of E2 and H2O2 for inducing apoptosis on rat vitronectin coated 8 well-chamber glass slides. After 24 h the cells were fixed and stained using a Cell Death Detection Kit (Roche Diagnostics, Inc., Tokyo, Japan) according to the manufacturer's instructions. For transwell migration assay, the NSCs (5×10^4) were seeded on 24 well-transwell plates and cultured with NSC proliferation medium for 6 h. Then, the cells were fixed and stained with DAPI followed by DAPI positive cell count under a fluorescent microscope in 5 randomly selected fields. The average number of migrated cells was evaluated as migration activity.

Preparation of CD31^{-} cells by FACS sorting

NSCs were incubated with FITC-conjugated anti-CD31 antibody (BD Pharmingen) for 30 min at 4 °C, and then DAPI solution (Sigma, 15000) was added and nuclei were stained for 10 min at RT for detecting dead cells. DAPI^{-}/CD31^{-} cells were further isolated using a FACS Aria machine (BD Biosciences) according to the manufacturer's instructions.

Sciatic nerve injury procedure

Unilateral nerve injury was induced in the sciatic nerves of 6-weeks-old C57BL/6 J female mice (Jackson laboratory) that underwent ovariectomy at 4 weeks of age. The animals were anesthetized with an intraperitoneal injection of ketamine (90–120 mg/kg) and xylazine (5–10 mg/kg) or with isoflurane anesthesia delivered at approximately 3 %, following which the sciatic nerve was exposed after surgical incision of the overlying skin and muscles. The nerve was crushed at the mid-thigh level for 15 s using a hemostat with tips covered by plastic tubing [22].

The mice were ovariectomized prior to sciatic nerve injury. Immediately following unilateral sciatic nerve crush injury, E2 (100 μg)-PLGA (10 mg) and/or NSC (1×10^5/mouse)-PLGA (10 mg) were applied on injured nerves in the treatment group, and treated with PLGA in the control group. PLGA was used as a carrier to insure long-lasting delivery. The muscles were then closed to prevent cell leakage, and the skin was closed with a surgical stapler. After surgery, animals were kept on a heating plate at 37 °C until they had recovered completely from anesthesia. All surgical procedures and animal care protocols were approved by the Northwestern University Animal Care and Use Committee.

Neurophysiological measurements

Nerve conduction studies were performed at the level of the sciatic and peroneal nerves using standard orthodromic surface recording techniques and a TECA TD-10 (Oxford Instruments, Pleasantville, NY) portable recording system in all sedated mice. Motor nerve parameters were assessed by placing two recording electrodes subcutaneously at the level of the sciatic notch and Achilles tendon, and the evoked electromyograms were recorded from the interosseous muscle of the foot. Compound muscle action potentials (CMAPs) were monitored by stimulating the peroneal nerve at the posterolateral ankle or by stimulating the sciatic nerve percutaneously with a monopolar needle electrode. Motor conduction velocity (MCV) was calculated by dividing the distance between stimulating electrodes by the average latency difference between the peaks of the CMAPs evoked from the two sites. Ten mice per group were studied at each time point. To consider intra-and interindividual variables that could influence conduction velocity measurements, such as ambient light and temperature, body temperature, and level of anesthesia, the ratio of the values between injured and uninjured nerves was used to present the results of MCV analyses. All measurements have been performed by investigators who were blinded to the assignment of experimental group. (Supplemental Figure 1).

Behavioral testing

Behavioral testing was performed weekly using the rotarod which were performed by 2 individuals blinded to mouse treatment status. In the rotarod test, the mice were placed on a rotarod treadmill, and the maximum duration on the device was calculated [23]. The speed was slowly increased from 4 to 40 rpm over a period of 10 min. The trial was ended if the animal fell off the rungs or gripped the device and spun around for 2 consecutive revolutions. The animals were trained 6 times for 2 weeks before sciatic nerve injury. The maximum duration (in seconds) on the rotarod treadmill was calculated using 3 taken 1 day before sciatic nerve injury. Motor test data are presented as the maximal duration.

In vivo assessment of regional nerve blood flow

After anesthesia, nerves were exposed by scalpel incision and blunt dissection of the overlying skin, muscle and connective tissue fascia, paying attention to do not disturb the sciatic nerve and its vasculature, then black sheet was insert under the nerve for exclude another tissue and enhance the contrast. Immediately after exposure of the nerves, the perfusion of vasa nervorum was assessed by laser Doppler flowmetry (PeriFlux System 5002, Perimed, Sweden). With this technique, an optic fiber probe is used to transmit the laser light to the tissue. When the laser light hits moving blood cells, it undergoes a change in wavelength. The magnitude and frequency distribution of these changes are directly related to the number and velocity of blood cells. Results are expressed in arbitrary Perfusion Units (PU). Measurements were performed bilaterally five times over the same region of interest. 5 or 6 animals were used for each time-point. Results are expressed as ratio between blood flow at the injured and contralateral uninjured nerve. This procedure allows rapid measurement of whole-nerve (epineurial and endoneurial) blood flow without protracted surgery. Nerve temperature was maintained at 34 °C ± 1 °C during the measurement period. To standardize regions of interest, we measured bilateral sides of surgically exposed whole nerve blood perfusion by Laser Doppler imaging system and the relative blood perfusion in injured nerve to that in contra-lateral side of intact nerve was examined.

Immunofluorescent staining

Sciatic nerves were fixed in 4 % paraformaldehyde, cryoprotected, and embedded in O.C.T. Tissue-Teck compound (SAKURA, Tokyo, Japan) and immediately frozen in liquid nitrogen. The cross-sections of sciatic nerves were cryosectioned at 5 μm thickness, collected on pre-cleaned superfrost slides (Fisher Scientific, Chicago IL, USA), dried for 1–2 h and stored at −80 °C. The slides were allowed to thaw, then were washed in PBS for 3 × 3 min. After that, the slides were blocked in 10 % donkey serum in PBS for 45 min. The slides were incubated in primary antibodies in blocking solution 2 h at 37 °C or overnight at 4 °C. We used anti-CD31 (PECAM-1) (1:50; BD Biosciences, San Jose, CA, USA), anti-BrdU (1:100; BD Biosciences), anti-GFP (1:150; GeneTex, Irvine, CA, USA). The slides were washed for 5 × 2 min in PBS, and then incubated with secondary antibodies diluted 1:250 in blocking solution for 1 h at room temperature in the dark. Slides were washed for 5 × 2 min in the dark, then incubated at room temperature for 10 min with DAPI and washed with 2 × 5 min in PBS. Slides were mounted with VECTASHIELD (Vector Laboratories, Burlingme, CA, USA) and analyzed on a Zeiss UV 510 Meta confocal microscope (Carl Zeiss).

Assessment for vascularity and cellular recruitment/proliferation in injured nerve

Vascularity was assessed by counting capillaries in injured sciatic nerves. The injured nerves were harvested at 4 weeks after injury for preparing cross-sections, which were stained by CD31. The CD31-positive cells were counted in the center portion of damaged sites in injured nerve histologically under a fluorescent microscope ($n = 5$ in each experimental group) and averaged. For assessment of cell recruitment, the number of locally administered DiI positive NSCs (1×10^5/mouse) was counted per entire nerve cross-section under a fluorescent microscope ($n = 5$ in each experimental group) and averaged.

In vivo cell proliferation activity was evaluated by counting BrdU positive cells in the center portion of damaged sites in injured nerve histologically. One week after nerve injury, BrdU (1 mg/mouse) was administered intraperitoneally 24 h prior to sacrifice and the nerves were harvested for cross-sectioning. The nerve was stained with anti-BrdU antibody to visualize the proliferating cells on sections. The BrdU injection experiment was performed on only mice with injured nerve and GFP-positive NSC administration. The BrdU-positive cell

numbers (/each cross section) were counted in each group ($n = 5$ in each experimental group) and averaged.

Statistical analysis

MCV, nerve blood flow, and vasa nervorum density are expressed as the ratio between injured and uninjured nerves and presented as the mean ± SEM. Group differences were analyzed by a nonparametric Student's *t* test (Mann–Whitney *U*), and comparisons between multiple groups were tested for significance via analysis of variance followed by post hoc testing with the Tukey procedure. Statistical analyses were performed with commercially available software (StatView™, Abacus Concepts, Berkeley, CA, USA). $P < 0.05$ was considered statistically significant.

Results

E2 promotes NSC functional activities

We examined the effect of E2 on NSCs cultured in vitro. An in vitro 3-(4,5-dimethylthiazol-2-yl)-5-(3-carboxymethoxyphenyl)-2-(4-sulfophenyl)-2H-tetrazolium) (MTS) proliferation assay revealed that E2 (1×10^{-7} and 1×10^{-8} mol/L) enhanced the proliferation of NSCs (1×10^{-7} mol/l, 1.365 ± 0.13 times 1×10^{-8} mol/l, 1.358 ± 0.23 times that in the control, $P < 0.01$) in the treatment groups; however, low-dose E2 did not have this effect (1×10^{-9} mol/l, 1 ± 0.05 times that in the control; Fig. 1a).

Apoptosis of NSCs was quantified by terminal deoxynucleotidyl transferase dUTP nick end labeling (TUNEL) staining (Fig. 1b). The mean number of TUNEL-positive NSCs per total number of NSCs (DAPI-stained nuclei) in the 1×10^{-7} and 1×10^{-8} mol/L E2 treatment groups was 12.5 ± 2.0 % and 26.5 ± 5.1 %, respectively. In contrast, the percentage of TUNEL-positive NSCs was substantially higher in the control group (42.5 % ± 9.7 %; $P = 0.0065$ vs. 1×10^{-7} mol/L E2 and $P = 0.0209$ vs. 1×10^{-8} mol/L E2). However, low-dose (1×10^{-9} mol/L) E2 did not prevent apoptosis (43.4 % ± 6.06 %). These results indicate that E2 prevents H_2O_2-induced NSC apoptosis in a concentration-dependent manner (Fig. 1b).

To understand the role of E2 in nerve recovery, we also examined its effect on the migration of NSCs. E2 mediated NSC migration in a concentration-dependent manner [1×10^{-7} M E2, 116.8 ± 21.1/high power field (HPF), $P < 0.01$ versus control; 1×10^{-8} M E2, 82.0 ± 11.8/HPF, $P < 0.05$ versus control; 1×10^{-9} M E2, 50.8 ± 21.9/HPF, no significant difference versus control; control, 26.8 ± 3.3/HPF]. Stromal cell-derived factor-1 (SDF-1; 100 ng/mL) was used as a positive control for NSCs migration (141.4 ± 18.1/HPF, $P < 0.01$ versus control; Fig. 1c).

We next examined the incorporation of NSCs into ECs in vitro. DiI-labeled NSCs and GFP-transfected human umbilical vein endothelial cells (HUVECs) were co-cultured for 12 h on Matrigel™. NSCs could incorporate into HUVEC tube junctions but not into formed tubes. Interestingly, E2 (1×10^{-8} M) enhanced NSC incorporation into the junctions as well as the tubes (black arrow); this enhancement was inhibited by ICI (Fig. 1d).

E2 promotes NSC differentiation into ECs

Previous studies of NSC differentiation in vitro have indicated that NSCs can differentiate into multiple lineages, including ECs [24]. To examine whether E2 could influence the differentiation fate of NSCs, we first studied the effects of E2 on the cultured cells. NSCs isolated from the brain contain a heterogeneous cell population that potentially includes ECs. This raises the possibility that NSCs positive for endothelial markers can represent EC

contamination of the NSC preparation instead of differentiated NSCs. To exclude this possibility, we investigated the effect of E2 on NSCs depleted of any cells expressing endothelial markers.

Flow cytometry analysis revealed that approximately 2.6 % of freshly isolated brain cells were positive for the endothelial marker CD31 (Fig. 2a). However, after 5 passages, the percentage of CD31-positive cells was decreased to 0.37 % (Fig. 2b). Cells were completely depleted of CD31-positive cells by flow cytometric sorting. The CD31-negative population was further cultured under conditions promoting EC differentiation in the presence or absence of E2. After 10 days, the proportion of CD31-positive cells was significantly increased in the E2 monotherapy group (5.69 %) compared with that in the control group (2.83 %), as demonstrated by both fluorescence-activated cell sorting analysis analysis (Fig. 2c) and immunocytochemical CD31 staining (control, 0.6 % ± 0.5 %; 1×10^{-8} mol/l E2, 2.8 % ± 0.8 %; $P < 0.05$). This effect was neutralized by ICI treatment (E2/ICI and ICI alone: 0 %; Fig. 2d and e). These results were further confirmed by culturing NSCs negatively selected for the presence of another endothelial lineage marker, isolectin B4 (ILB4). After 10 days of culture under the endothelial cell differentiation conditions, cells that did not express ILB4 originally began to express the endothelial marker. Similar to the CD31-negative cells, cells treated with E2 contained a significantly larger number of ILB4-positive cells (5.1 ± 0.8 %) compared with the control cells (2.3 ± 0.1 %; $P = 0.0019$). Furthermore, the ability of E2 to promote the differentiation of NSCs into ECs was completely inhibited by ICI, an estrogen receptor antagonist, suggesting that the effect of E2 on NSC differentiation is mediated through estrogen receptor (Fig. 2d and f). We also checked the mRNA levels of Jagged-1, neuropilin 1, VEGF-B, and ephrin B2 in NSCs by cDNA microarray analysis (Oligo GEArray® Mouse Angiogenesis Microarray, OMM-024, SABioscience™). These mRNA in NSC were upregulated in the presence of E2 (1×10^{-8} mol/L) compared with those in the absence of E2 (Supplemental Table 1).

Next, we hypothesized that E2 improves nerve recovery after crush injury, at least in partial, by promoting the differentiation of NSCs into ECs and accelerating angiogenesis. To examine whether NSCs can give rise to ECs in vivo, we examined the differentiation potential of DiI-labeled NSCs grown in vitro and transplanted into mice following nerve crush injury. Differentiation was evaluated by CD31 staining.

Next, we confirmed whether NSCs could differentiate into ECs in vivo. The injured sciatic nerves of mice were treated with DiI-labeled NSC (1×10^5/50 μL)-PLGA and E2-PLGA or DiI-labeled NSC (1×10^5/50 μL)-PLGA alone. Fourteen days after injury, the mice were also injected intracardially with ILB4. Then we examined the whole mount sciatic nerves by confocal microscopy. There were vessel-like structures stained by DiI and ILB4 near the original vessels (Fig. 3a). Only a few CD31-positive DiI-labeled NSCs were located in the epineural area in the NSC monotherapy group 14 days after injury. Conversely, there were several DiI-positive cells stained by CD31 in the epineural and endoneural areas in the combination therapy group (Fig. 3b). The number of CD31-positive DiI-stained NSCs was higher in the combination therapy group than in the NSC monotherapy group (6.2 ± 1.9/cross-section vs. 1.4 ± 0.5/cross-section, respectively, $P < 0.05$; Fig. 3c).

Local E2/PLGA administration does not increase serum E2 concentrations

We first compared the serum E2 concentration among the following groups; (1) E2 local administration with E2-PLGA (E2-PLGA group), (2) E2 systemic administration by E2-pellet implantation (E2-pellet group), and (3) placebo-pellet implantation (placebo-pellet group). The serum E2 concentration was significantly increased in the E2-pellet group compared with the other two groups, however, the E2-PLGA group showed low serum E2 concentration similar to that in the placebo-pellet implantation group resulting in no

significant difference of serum E2 concentration between the two groups. (Supplemental Figure 4).

Nerve functional recovery following E2/NSC combination therapy

MCV was undetectable immediately after nerve injury. A partial recovery of nerve function was observed on day 7 after injury in all treatment groups, with no significant difference between different treatments. However, on day 14, animals treated with NSC/E2 combination therapy exhibited significantly improved recovery compared with the control group (MCV ratios: 0.89 ± 0.26 and 0.40 ± 0.33, respectively; $P = 0.03$). Twenty-eight days after injury, both monotherapy groups exhibited better recovery than the control group (MCV ratios: control, 0.42 ± 0.26; NSC, 0.98 ± 0.16; $P = 0.029$ vs. control; E2, 0.78 ± 0.06; $P = 0.003$ vs. control). However, the combination therapy group still resulted in a significantly higher MCV ratio (1.30 ± 0.20) compared with the monotherapy groups ($P = 0.0006$ vs. E2, $P = 0.0243$ vs. NSC, $P = 0.0003$ vs. control; Fig. 4a).

Nerve functional recovery was also evaluated by nerve voltage measurements. Similar to MCV, nerve function did not begin to recover until 7 days after injury in all treatment groups. After 14 days, both monotherapy (3.26 ± 0.52 mV) and combination (5.12 ± 0.80 mV) therapy resulted in higher amplitude compared with the control therapy (1.74 ± 1.09 mV; $P = 0.0226$ and $P = 0.0005$, respectively). Twenty-eight days after injury, animals treated with NSC/E2 combination therapy (6.86 ± 1.48 mV) had a higher voltage amplitude compared with the other treatment groups (control, 2.7. ± 1.48 mV; E2, 3.23 ± 1.00 mV; NSC, 4.42 ± 0.28 mV; $P = 0.0028$, $P = 0.0041$, and $P = 0.067$, respectively; Fig. 4b).

Next, the effect of different treatment regimens on the recovery of motor coordination after nerve injury was assessed by the duration of exercise on the rotarod treadmill. The analysis failed to detect a difference between the control group (376.8 ± 68.0 ms) and both monotherapy groups (E2, 428.6 ± 118.2 ms; NSC, 437.6 ± 124.9 ms). In contrast, animals treated with NSC/E2 combination therapy completely recovered their ability to perform the rotarod task for the maximum allowed exercise time of 600 ms ($P < 0.05$ vs. all other groups; Fig. 4c).

Increased vascularity and cell proliferation in injured nerve following E2/NSC combination therapy

We found that at 4 weeks after injury, the number of capillaries was significantly increased in the monotherapy groups in both the epineural (control, 10.7 ± 2.1; NSC, 27.0 ± 6.6; E2, 60.7 ± 11.0; $P \leq 0.05$ vs. control) and endoneural (control, 11.7 ± 2.5; NSC, 21.7 ± 2.1; E2, 19.3 ± 1.5; $P \leq 0.05$ vs. control) areas. E2 treatment was more effective for epineural angiogenesis. Combination therapy resulted in higher capillary numbers in both the epineural (96.3 ± 6.1) and endoneural areas (29.0 ± 1.7) compared with monotherapy (epineural: $P = 0.0002$ vs. NSC and $P = 0.0080$ vs. E2; endoneural: $P = 0.0094$ vs. NSC and $P = 0.0019$ vs. E2; Fig. 5a–c). Consistent with the result of capillary density, nerve blood perfusion assessed by Laser Doppler imaging system was also significantly improved in the E2/NSC combination therapy group compared with the other groups. (Supplemental Fig. 2a–c).

Next, cell proliferation was measured by bromodeoxyuridine (BrdU) staining 7 days after nerve injury. The number of proliferating cells was significantly increased in both the E2- and the NSC-treated groups compared with that in control group (control, 19.6 ± 2.19/cross-section; NSC, 43.2 ± 3.57/cross-section; E2, 58.2 ± 7.50/cross-section; $P \leq 0.05$ vs. control). The highest number of proliferating cells inside the recovering nerve was found in the animals treated with combination therapy (NSC/E2, 76.8 ± 4.08; $P \leq 0.05$ vs. control, NSC

alone, and E2 alone). E2 monotherapy resulted in a greater number of proliferating cells compared with NSC monotherapy ($P < 0.05$; Fig. 5d and e). The result indicates that locally released E2 promoted recruited NSC proliferation in injured nerve.

E2 augments the transplanted nsc recruitment to injured nerve promoting the proliferation activity

We examined NSC localization 7 days after nerve injury with cell transplantation. We observed DiI-labeled NSCs mainly around the sciatic nerve in NSC-treated mice. The number of NSCs localized in the injured nerves was higher in the combination therapy group than in the NSC monotherapy group (Fig. 6a).

To compare the incorporation of NSCs into the injury site, animals were treated with NSCs isolated from mice constitutively expressing eGFP. Seven days after injury, an increased number of GFP-positive cells was observed at the injury site of mice treated with both E2 and NSC (E2, 57.7 ± 7.6; NSC, 8.0 ± 2.6; $P = 0.0004$). Although the number of incorporated cells decreased 14 days after injury in both groups, the combination therapy group retained significantly more GFP-positive cells compared with the NSC monotherapy group (NSC/E2, 19.3 ± 5.7; NSC, 1.3 ± 0.6; $P = 0.0055$; Fig. 6b and c). Proliferating NSCs were also detected by BrdU staining. E2 enhanced NSC proliferation (NSC, 2.8 ± 1.79; NSC/E2, 10.4 ± 2.60; $P = 0.014$) 7 days after injury (Fig. 6b and d).

Discussion

A major finding of this study is that NSCs and E2 revert functional deficits by enhancing neovascularization in mouse sciatic nerve injury models. As early as 14 days after injury, the impairments in exploratory behavior and motor activity observed in injured mice were less severe in mice that received E2 or NSC monotherapy than in the controls. This protective effect was also observed throughout the post-treatment period. Moreover, we also observed that in the NSC/E2 combination therapy group, the hindlimb function of the injured mice was similar to that of uninjured mice at 4 weeks after injury.

Neurogenesis in injured nerves reportedly requires angiogenesis approximately 7 days after injury [25], indicating that angiogenesis is a critical part of neurogenesis. Indeed, NSC/E2 combination therapy resulted in higher capillary numbers in the epineural and endoneural areas at 4 weeks after injury. It also resulted in optimal blood perfusion in injured nerves. Interestingly, NSC monotherapy increased endoneural vascularity by a greater extent compared with E2 monotherapy, whereas E2 monotherapy increased epineural vascularity by a greater extent compared with NSC monotherapy. These findings may be attributed to the migration of NSCs into the nerve, following which they released several angiogenic cytokines, such as vascular endothelial growth factor (VEGF), neural growth factor, and SDF-1. Conversely, E2-PLGA treatment primarily affected fibroblast-containing areas outside the nerve.

We observed several beneficial effects of NSC/E2 combination therapy. First, we observed that substantial numbers of injected NSCs migrated into the injured nerves after combination therapy. In contrast, the injected NSCs localized around the nerve after NSC monotherapy, and the number of NSCs was lower than that after NSC/E2 combination therapy, suggesting that E2 could enhance the proliferation and migration of NSCs into the nerve and prevent NSC apoptosis. Our laboratory previously reported that E2 enhanced the proliferation [16] and migration [26] of progenitor cells and prevented their apoptosis [27]. Indeed, we observed the same effect of E2 on NSC function in vivo and in vitro. The enhanced biological activities of NSCs, such as proliferation, migration, anti-apoptosis, and differentiation, which were stimulated by E2, were blocked by a nonselective estrogen

receptor antagonist ICI; this finding supported the fact that these promotional effects of E2 were caused by functional E2-ER (estrogen receptor) binding. Indeed, we confirmed that NSCs express both ER alpha and ER beta (ER alpha < ER beta) genes by RT-PCR analysis (Supplemental Figure 3).

Second, we observed that NSCs could differentiate into ECs both in vivo and in vitro, and the NSCs were present in functional vessels at 4 weeks after injury. Notably, E2 enhanced the differentiation of NSCs into ECs both in vivo and in vitro. Previously, Wurmser et al. [13] reported that NSCs could differentiate into both neurons and ECs in an in vitro model. Recently, Ii et al. [24] also confirmed the differentiation of NSCs into ECs using an in vivo model. However, because NSCs are an originally heterogeneous population, the brain-derived stem/progenitor cells in our study, which were the initial cell population of neurospheres, contained approximately 2.5 % CD31-positive cells derived from cerebral vessels, even after several passages. We therefore needed to exclude the initial contamination of CD31-positive cells in neurospheres to confirm that NSCs actually differentiated into ECs. We eventually confirmed that CD31-negative NSCs could differentiate into ECs in EC differentiation medium supplemented with growth factors. Moreover, the differentiation of NSCs into ECs in the presence of E2 was approximately twofold that in the absence of E2. Although the differentiation of neural progenitor cells into ECs is not clearly understood, several growth factors/cytokines have been identified as vital for this differentiation. To explore the mechanism by which E2 enhances NSC function and to analyze the changes in the damaged tissue environment, we aimed to elucidate certain angiogenesis-related factors in NSCs by cDNA microarray analysis. The mRNA levels of Jagged-1, neuropilin 1, VEGF-B, and ephrin B2 in NSCs were upregulated in the presence of E2 (1×10^{-8} mol/L) compared with those in the absence of E2 (Supplemental Table 1), suggesting that these upregulated genes are involved in E2-induced NSC differentiation into endothelial lineages.

In conclusion, the findings of this study revealed that NSCs could differentiate into ECs in vivo and in vitro despite their known heterogeneity. Apparently, E2 enhanced the function of NSCs and accelerated their differentiation into ECs. Because the local administration of E2 with PLGA results in low E2 serum concentrations (Supplemental Figure 4) we can avoid the side effects of systemic E2 administration, such as breast or uterine carcinogenesis. In addition, since NSCs are immunologically tolerant compared with matured brain-derived cells [28], it may be possible to perform allogeneic NSC transplantation therapy in clinical settings as long as the safety is guaranteed. The combination of E2 and NSCs could be therefore useful for the treatment of nerve injury, specifically, in men and menopausal women with low serum E2 level.

Supplementary Material

Refer to Web version on PubMed Central for supplementary material.

Acknowledgments

We thank W. Kevin Meisner, PhD, ELS, for editorial support and A. Peterson for administrative assistance. This study was supported in part by NIH grants HL-53354, HL-57516, HL-77428, HL-63414, HL-80137, and PO1HL-66957.

References

1. Behl C. Oestrogen as a neuroprotective hormone. Nat Rev. 2002; 3(6):433–442.

2. Singer CA, Figueroa-Masot XA, Batchelor RH, Dorsa DM. The mitogen-activated protein kinase pathway mediates estrogen neuroprotection after glutamate toxicity in primary cortical neurons. J Neurosci. 1999; 19(7):2455–2463. [PubMed: 10087060]

3. Behl C, Skutella T, Lezoualc'h F, Post A, Widmann M, Newton CJ, Holsboer F. Neuroprotection against oxidative stress by estrogens: structure-activity relationship. Mol Pharmacol. 1997; 51(4): 535–541.

4. Hurn PD, Macrae IM. Estrogen as a neuroprotectant in stroke. J Cereb Blood Flow Metab. 2000; 20(4):631–652. [PubMed: 10779008]

5. Roof RL, Hall ED. Gender differences in acute CNS trauma and stroke: neuroprotective effects of estrogen and progesterone. J Neurotrauma. 2000; 17(5):367–388. [PubMed: 10833057]

6. Pallini R, Vitiani LR, Bez A, Casalbore P, Facchiano F, Di Giorgi Gerevini V, Falchetti ML, Fernandez E, Maira G, Peschle C, Parati E. Homologous transplantation of neural stem cells to the injured spinal cord of mice. Neurosurgery. 2005; 57(5):1014–1025. discussion 1014–1025.

7. Bez A, Corsini E, Curti D, Biggiogera M, Colombo A, Nicosia RF, Pagano SF, Parati EA. Neurosphere and neurosphere-forming cells: morphological and ultrastructural characterization. Brain Res. 2003; 993(1–2):18–29. [PubMed: 14642827]

8. McKay R. Stem cells in the central nervous system. Science. 1997; 276(5309):66–71. [PubMed: 9082987]

9. Gage FH. Mammalian neural stem cells. Science. 2000; 287(5457):1433–1438. [PubMed: 10688783]

10. Cao Q, Benton RL, Whittemore SR. Stem cell repair of central nervous system injury. J Neurosci Res. 2002; 68(5):501–510. [PubMed: 12111840]

11. Pluchino S, Zanotti L, Rossi B, Brambilla E, Ottoboni L, Salani G, Martinello M, Cattalini A, Bergami A, Furlan R, Comi G, Constantin G, Martino G. Neurosphere-derived multipotent precursors promote neuroprotection by an immunomodulatory mechanism. Nature. 2005; 436(7048):266–271. [PubMed: 16015332]

12. Lindvall O, Kokaia Z, Martinez-Serrano A. Stem cell therapy for human neurodegenerative disorders-how to make it work. Nat Med. 2004; 10(Suppl):S42–S50. [PubMed: 15272269]

13. Wurmser AE, Nakashima K, Summers RG, Toni N, D'Amour KA, Lie DC, Gage FH. Cell fusion-independent differentiation of neural stem cells to the endothelial lineage. Nature. 2004; 430(6997):350–356. [PubMed: 15254537]

14. Krasinski K, Spyridopoulos I, Asahara T, van der Zee R, Isner JM, Losordo DW. Estradiol accelerates functional endothelial recovery after arterial injury. Circulation. 1997; 95(7):1768–1772. [PubMed: 9107161]

15. Iwakura A, Shastry S, Luedemann C, Hamada H, Kawamoto A, Kishore R, Zhu Y, Qin G, Silver M, Thorne T, Eaton L, Masuda H, Asahara T, Losordo DW. Estradiol enhances recovery after myocardial infarction by augmenting incorporation of bone marrow-derived endothelial progenitor cells into sites of ischemia-induced neovascularization via endothelial nitric oxide synthase-mediated activation of matrix metalloproteinase-9. Circulation. 2006; 113(12):1605–1614. [PubMed: 16534014]

16. Hamada H, Kim MK, Iwakura A, Ii M, Thorne T, Qin G, Asai J, Tsutsumi Y, Sekiguchi H, Silver M, Wecker A, Bord E, Zhu Y, Kishore R, Losordo DW. Estrogen receptors alpha and beta mediate contribution of bone marrow-derived endothelial progenitor cells to functional recovery after myocardial infarction. Circulation. 2006; 114(21):2261–2270. [PubMed: 17088460]

17. Islamov RR, Hendricks WA, Jones RJ, Lyall GJ, Spanier NS, Murashov AK. 17Beta-estradiol stimulates regeneration of sciatic nerve in female mice. Brain Res. 2002; 943(2):283–286. [PubMed: 12101051]

18. Wilson ME, Liu Y, Wise PM. Estradiol enhances Akt activation in cortical explant cultures following neuronal injury. Brain Res Mol Brain Res. 2002; 102(1–2):48–54. [PubMed: 12191493]

19. Otsuka M, Uenodan H, Matsuda Y, Mogi T, Ohshima H, Makino K. Therapeutic effect of in vivo sustained estradiol release from poly (lactide-co-glycolide) microspheres on bone mineral density of osteoporosis rats. Bio-Med Mater Eng. 2002; 12(2):157–167.

20. Okabe M, Ikawa M, Kominami K, Nakanishi T, Nishimune Y. 'Green mice' as a source of ubiquitous green cells. FEBS Lett. 1997; 407(3):313–319. [PubMed: 9175875]

21. Takeuchi H, Natsume A, Wakabayashi T, Aoshima C, Shimato S, Ito M, Ishii J, Maeda Y, Hara M, Kim SU, Yoshida J. Intravenously transplanted human neural stem cells migrate to the injured spinal cord in adult mice in an SDF-1- and HGF-dependent manner. Neurosci Lett. 2007; 426(2): 69–74. [PubMed: 17884290]

22. De Koning P, Brakkee JH, Gispen WH. Methods for producing a reproducible crush in the sciatic and tibial nerve of the rat and rapid and precise testing of return of sensory function. Beneficial effects of melanocortins. J Neurol Sci. 1986; 74(2–3):237–246. [PubMed: 3016200]

23. Jeong SW, Chu K, Jung KH, Kim SU, Kim M, Roh JK. Human neural stem cell transplantation promotes functional recovery in rats with experimental intracerebral hemorrhage. Stroke J Cereb Circul. 2003; 34(9):2258–2263.

24. Ii M, Nishimura H, Sekiguchi H, Kamei N, Yokoyama A, Horii M, Asahara T. Concurrent vasculogenesis and neurogenesis from adult neural stem cells. Circ Res. 2009; 105(9):860–868.10.1161/CIRCRESAHA.109.199299 [PubMed: 19762683]

25. Pola R, Aprahamian TR, Bosch-Marce M, Curry C, Gaetani E, Flex A, Smith RC, Isner JM, Losordo DW. Age-dependent VEGF expression and intraneural neovascularization during regeneration of peripheral nerves. Neurobiol Aging. 2004; 25(10):1361–1368.10.1016/j.neurobiolaging.2004.02.028 [PubMed: 15465634]

26. Iwakura A, Luedemann C, Shastry S, Hanley A, Kearney M, Aikawa R, Isner JM, Asahara T, Losordo DW. Estrogen-mediated, endothelial nitric oxide synthase-dependent mobilization of bone marrow-derived endothelial progenitor cells contributes to reendothelialization after arterial injury. Circulation. 2003; 108(25):3115–3121. [PubMed: 14676142]

27. Koga M, Hirano K, Hirano M, Nishimura J, Nakano H, Kanaide H. Akt plays a central role in the anti-apoptotic effect of estrogen in endothelial cells. Biochem Biophys Res Commun. 2004; 324(1):321–325. [PubMed: 15465021]

28. Holan V, Lipoldova M, Zajicova A. Immunological non-reactivity of newborn mice: immaturity of T cells and selective action of neonatal suppressor cells. Cell Immunol. 1991; 137(1):216–223. [PubMed: 1832088]

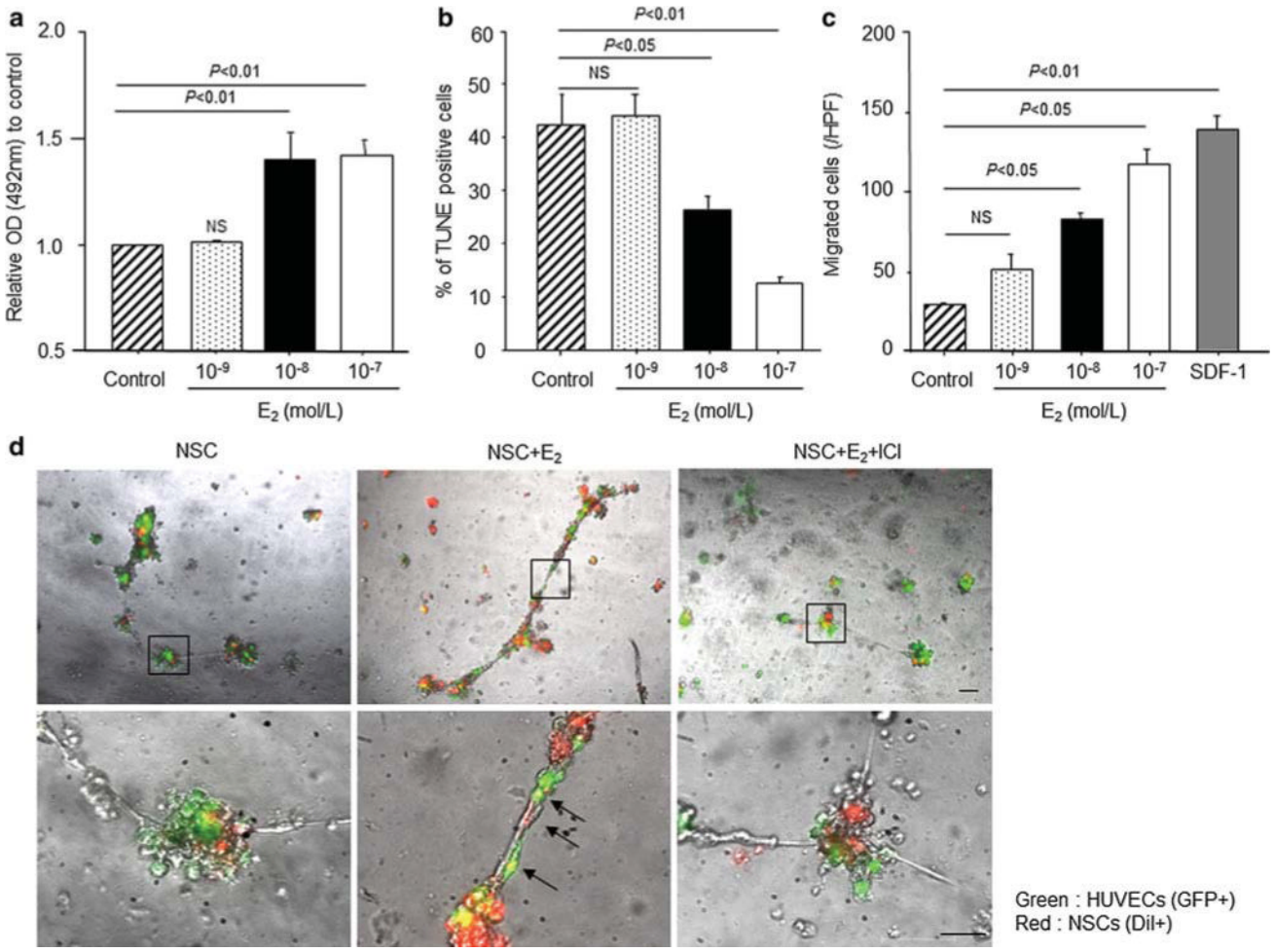

Fig. 1.

NSC function assays. **a** Proliferation assay. The proliferation activity of NSCs was evaluated as optical density for MTS dye reacted with viable cells. Y-axis shows optical density (OD) at 492 nm. NS, no significant change. **b** Apoptosis assay. The cell apoptosis was evaluated as the percent of TUNEL positive cells in total cells. Y-axis shows the percentage of apoptotic (TUNEL positive) cells in high power field. *NS* no significant change. **c** Transwell migration assay. The migration activity was evaluated as the number of migrated cells to the lower side of the membrane. Y-axis shows the number of migrated cells in high power field (HPF). *NS* no significant change. **d** NSC vasculogenesis assay. DiI-labeled NSCs (*red*) were co-cultured with GFP-transfected HUVECs (*green*) on Matrigel™ for 12 h. The *black arrows* show NSC incorporation into the HUVEC-derived tube. The *squares* in the upper panels were magnified in the lower panels. *Scale bar* = 10 μm. (Color figure online)

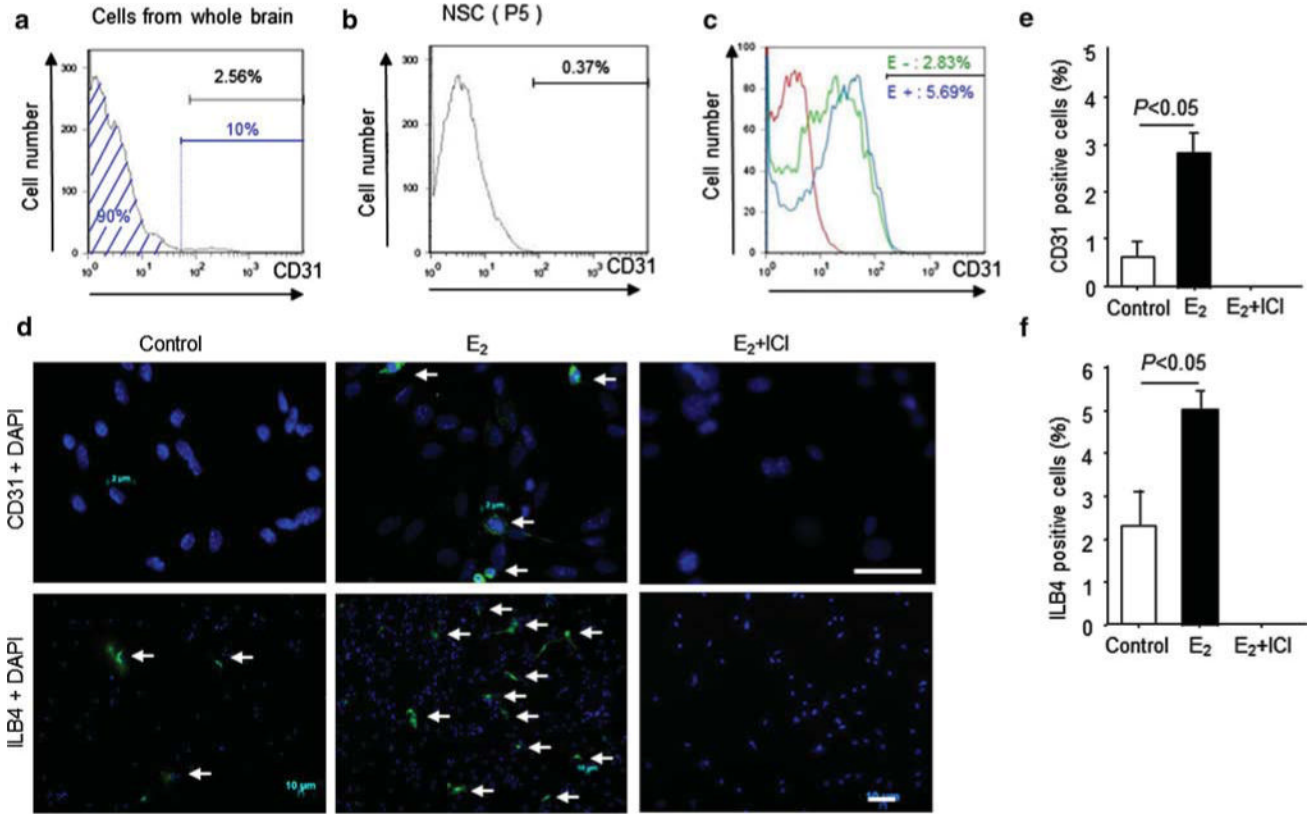

Fig. 2.

NSC differentiation capacity to endothelial cell in vitro **a** The *black bar* shows the percent of CD31-positive cells (2.56 %). The CD31-negative cells (90.08 %), represented by the *blue area*, were sorted by FACS. **b** and **c** The FSCS-sorted CD31-negative cells were further cultured in NSC proliferation medium or EBM2 medium. **b** The *bar shows* the percentage of CD31-positive cells (0.37 %) after 5 passages of CD31-negative cells with NSC proliferation medium. **c** The *red line* represents the isotype control, the *green line* represents the histogram of CD31-negative cells after 10 days in culture with EBM2, and the *blue line* represents the histogram of CD31-negative cells after 10 days in culture with EBM2 in the presence of E2 (1×10^{-8} M). **d**, **e**, and **f**, After 10 days in culture of CD31- or ILB4-negative cells with EBM2 medium in the presence or absence of E2, the cells were stained with an anti-CD31 antibody or ILB4 and counted under a fluorescent microscopy. **d** The *arrows* indicate CD31-positive NSCs in the upper panels and ILB4-positive NSCs in the lower panels. *Scale bars* = 5 μm (for upper panels) and 50 μm (for lower panels). **e** Y-axis shows the percentage of CD31-positive cells in high power field. **f** Y-axis shows the percentage of ILB4-positive cells in high power field. (Color figure online)

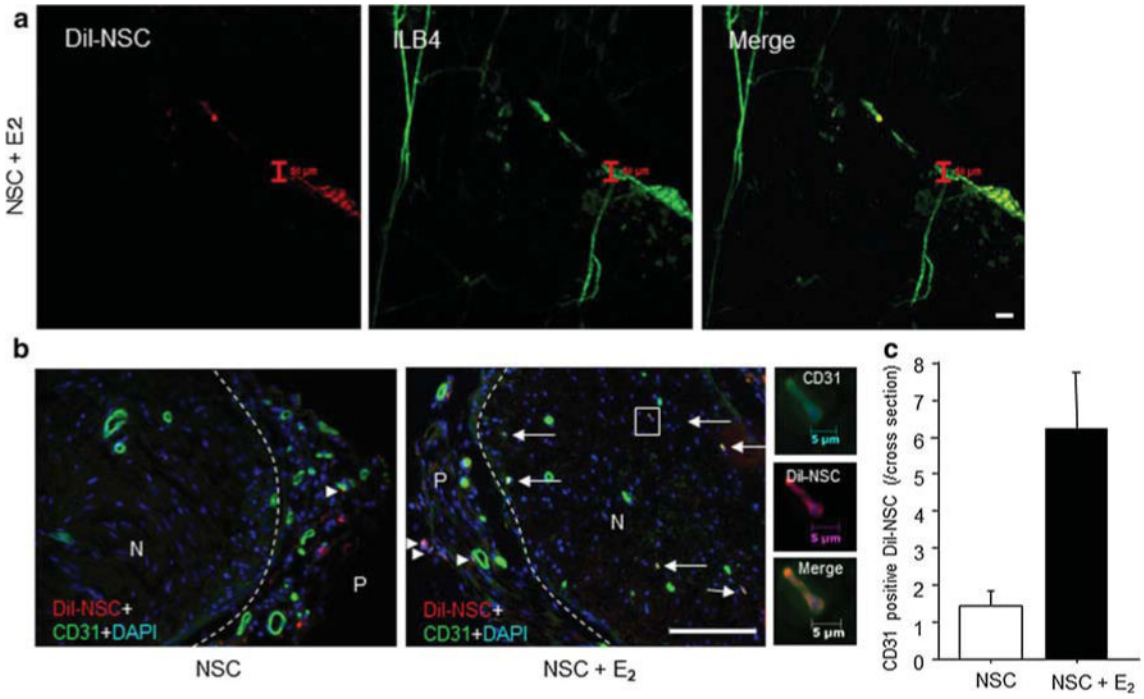

Fig. 3.

NSC differentiation to EC in vivo. **a** Whole mount staining of sciatic nerve on day 14 after injury. After nerve crush injury, the injured nerves of mice were treated with DiI-NSC (5×10^5) injection and E2-PLGA. The red color shows DiI-labeled NSCs, and the green color shows ILB4-positive vessels. *Scale bar* = 50 μm. **b**, Cross-section of injured nerve exhibits CD31-positive cells in NSCs 28 days after injury. GFP-NSCs with/without E2 were administered to the injury site immediately after crush injury, and the sciatic nerve of each mouse was harvested 28 days after injury. The green color shows CD31-positive cells (NSCs), and the red color shows DiI-labeled NSCs. *N* nerve and *P* perineurium. The *arrows* denote CD31-positive NSCs inside the nerve, and the *arrowheads* denote DiI/CD31-double positive NSCs in perineural area. *Scale bar* = 100 μm. **c** CD31-positive DiI-labeled NSCs were counted under a fluorescent microscopy. Y-axis shows the number of CD31-positive DiI-labeled NSCs in entire nerve cross-section

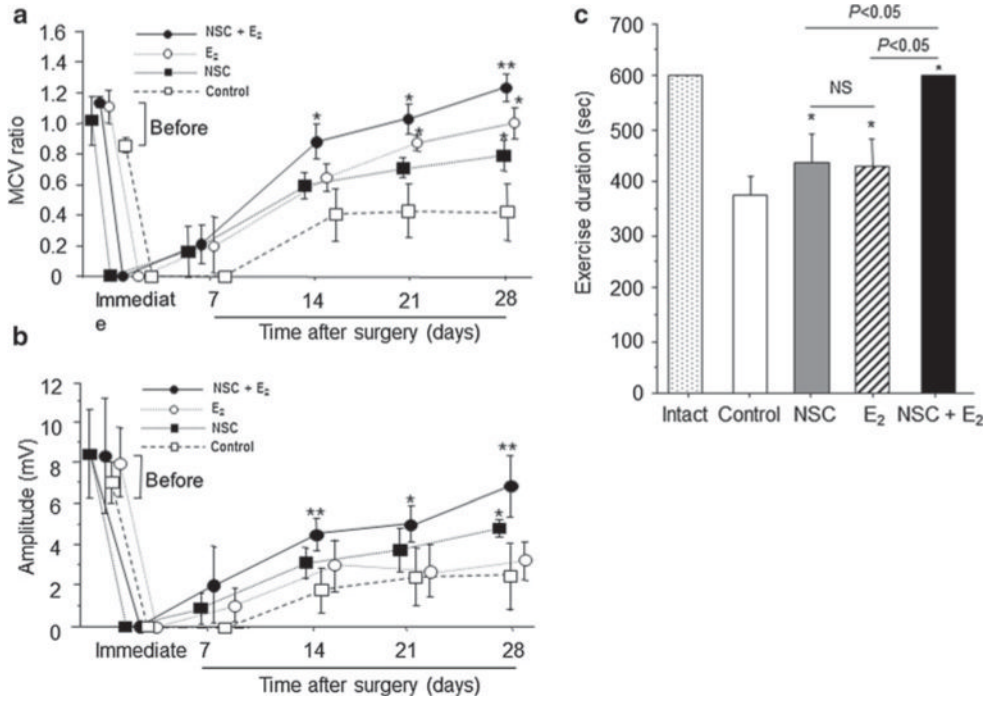

Fig. 4.

Physiological and functional recovery in injured sciatic nerve by E2 treatment. **a** and **b** Motor nerve conduction velocity (m/s) and nerve voltage amplitude (mV) were measured in injured sciatic nerves weekly for up to 4 weeks after nerve crush injury. E2: E2 (100 μg) + PLGA (10 mg), NSC: NSCs (1×10^6) + PLGA (10 mg), and NSCs + E2 : NSCs (1×10^6) + E2 (100 μg) + PLGA (10 mg), and Control: PLGA (10 mg) alone were locally administered to sites of injury. ($n = 5$ in each experimental group) *, $P < 0.05$ versus no treatment; **, $P < 0.05$ versus control, NSC, and E2 groups. **c** Nerve functional recovery was assessed by Rotarod testing. Exercise duration was measured in each group ($n = 5$) at 4 weeks after injury. All animals practiced running on the Rotarod before injury, and exercise duration was assessed 1, 2, 3, and 4 weeks after surgery. The sham-operated animals with intact nerves were used as a control (Intact) group in addition to the same groups used for MCV measurement. *$P < 0.05$ versus control

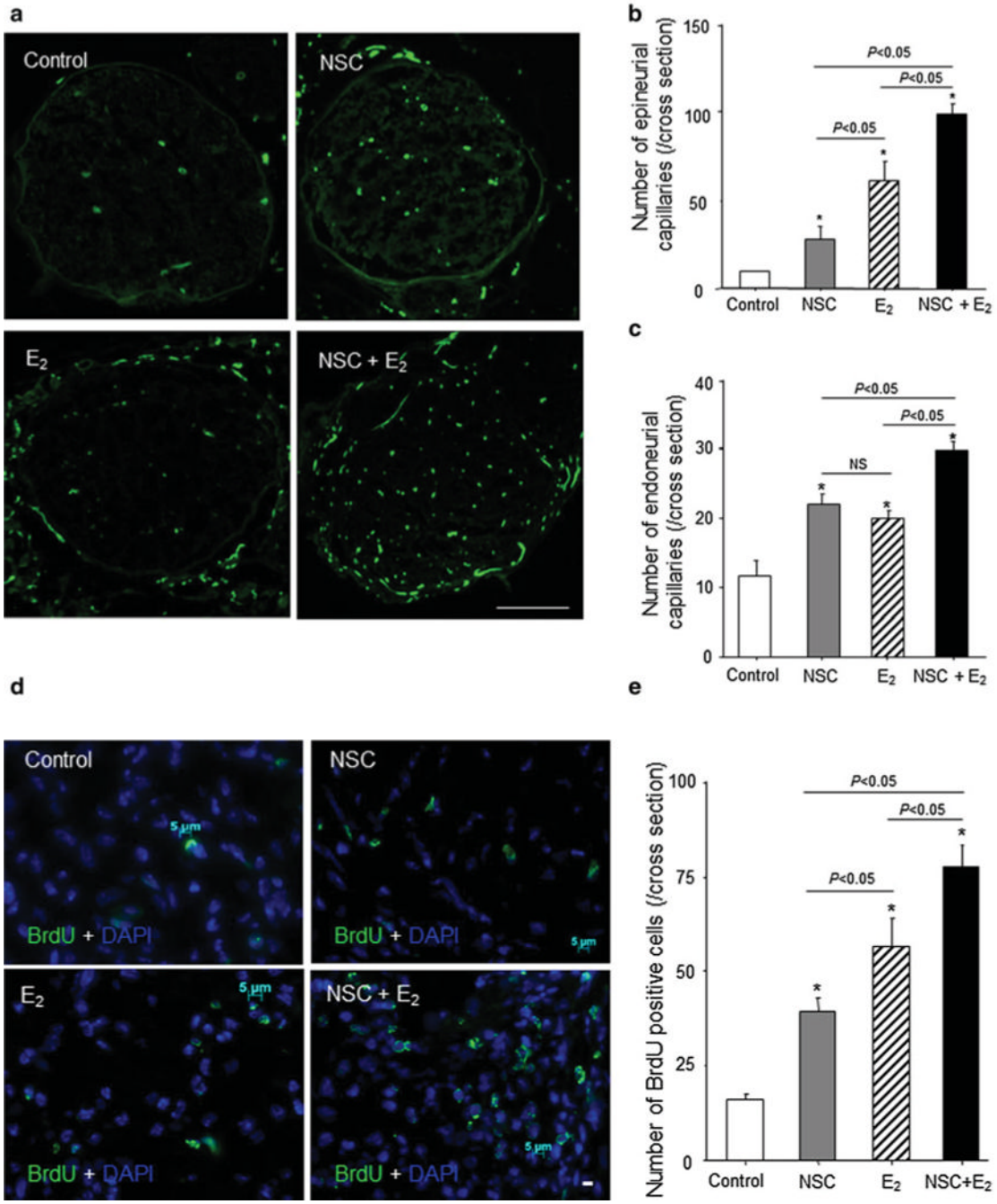

Fig. 5.

Intraneural neovascularization and cell proliferation after nerve crush injury. The sciatic nerves from injured mice were harvested 4 weeks after surgery for preparing cross-sections, which were examined by immunofluorescent staining for CD31. **a** The *green shows* CD31-positive capillaries. ($n = 5$ in each experimental group) *Scale bar* = 500 μm. **b** and **c** The graph shows capillary density in nerve cross-sections. The number of epineurial (b) and endoneurial (c) CD31-positive capillaries was counted in the same samples by fluorescent microscopy. *$P < 0.05$ versus control. **d** and **e**. The cell proliferation in injured nerve was evaluated by immunofluorescent staining for BrdU 1 week after surgery. Before 24 h prior

to sacrifice, BrdU (1 mg/mouse) was administered intraperitoneally in each group ($n = 5$) **d** The *green* and *blue* represent BrdU-positive cells and DAPI-positive nuclei, respectively. *Arrows* indicate *green* and *blue* double-positive cells. *Scale bar* = 5 μm. **e** The BrdU-positive cell numbers were counted in each group. ($n = 5$ in each experimental group) Y-axis represents the number of BrdU-positive cells in entire cross-sections. *$P < 0.05$ versus control. (Color figure online)

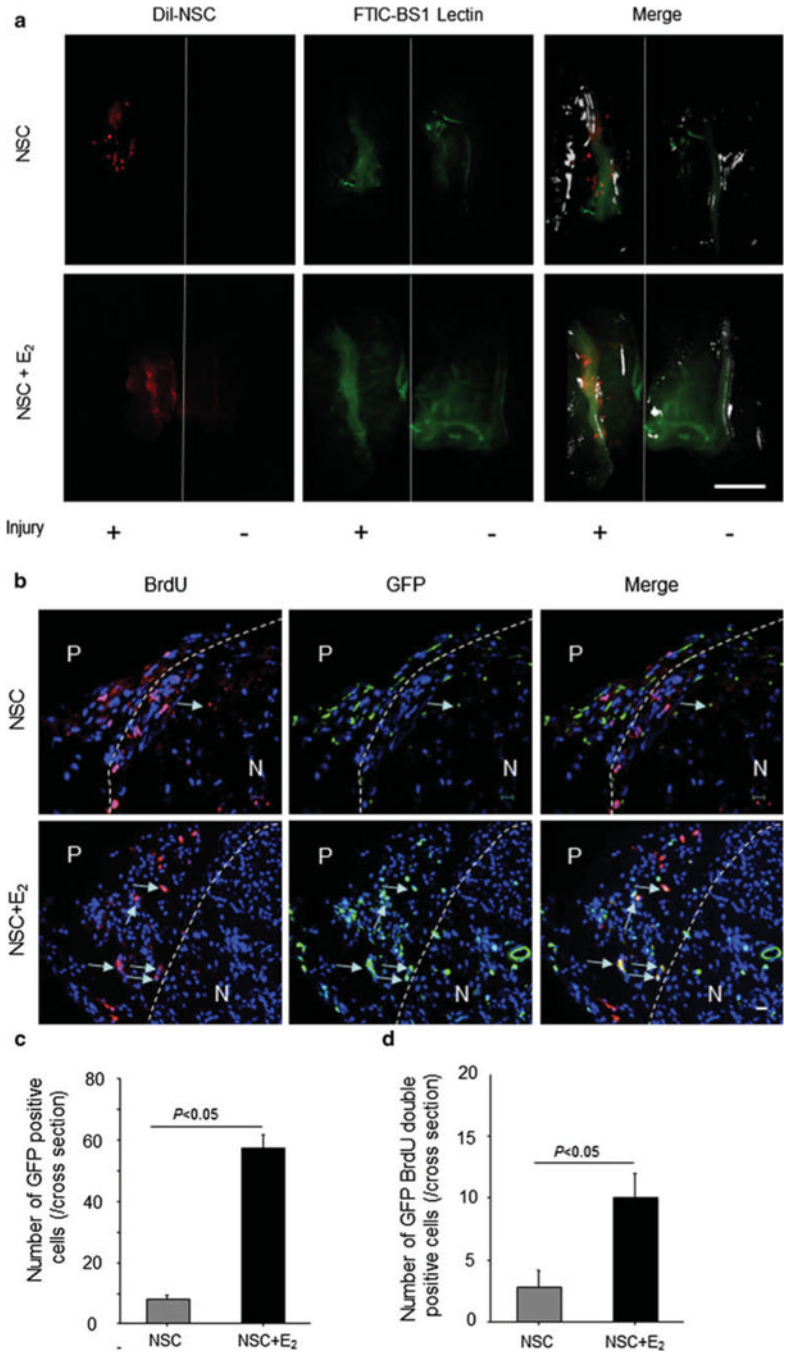

Fig. 6.

NSC incorporation into injured nerve. **a** The mice were anesthetized and injected with FITC-BS1 lectin via a tail vein. Fifteen minutes after injection, the back skin was removed from the body in each mouse, and the mice were scanned by in vivo imaging (OV100) at 7 days after surgery. The *red shows* DiI-labeled NSCs, and the green shows functional vascular staining. *Scale bar* = 5 mm. **b** The sciatic nerves were harvested 7 days after injury and stained with an antibody for GFP immunohistochemically. The green shows recruited NSCs isolated from GFP mice. *Arrows*, GFP and BrdU double positive NSCs. *P* perineurium; *N* nerve. *Scale bar* = 10 μm. **c** The *graph* shows the number of GFP-positive

cells in entire nerve cross-sections. The *gray bar* represents the results in NSC monotherapy group (NSC), and the *black bar* represents the results in NSC/E2 combination therapy group (NSC + E_2). (n = 5 in each experimental group). **d** Quantification of GFP and BrdU double-positive cells in entire nerve cross-sections. The *gray bar* represents the results in NSC monotherapy group (NSC), and the *black bar* represents the results in NSC/E2 combination therapy group (NSC + E_2). (n = 5 in each experimental group). (Color figure online)